Modification of the Nanoscale Structure of the J-Aggregate of a Sulfonate-Substituted Amphiphilic Carbocyanine Dye through Incorporation of Surface-Active Additives

Hans von Berlepsch,*,† Stefan Kirstein,‡ Ralph Hania,§ Audrius Pugžlys,§,|| and Christoph Böttcher†

Forschungszentrum für Elektronenmikroskopie der Freien Universität Berlin, Fabeckstrasse 36 a, D-14195 Berlin, Germany, Institut für Physik, Humboldt Universität zu Berlin, Newtonstrasse 15, D-12489 Berlin, Germany, and Materials Science Center, University of Groningen, Nijenborgh 4, 9747AG Groningen, The Netherlands

Received: September 7, 2006; In Final Form: December 20, 2006

The amphiphilic dye 3,3′-bis(2-sulfopropyl)-5,5′,6,6′-tetrachloro-1,1′-dioctylbenzimidacarbocyanine (C8S3) self-aggregates in aqueous solution to form tubular J-aggregates with a diameter of 17.0 ± 0.5 nm, a wall thickness of ∼4 nm, and a length exceeding several hundred nanometers. The absorption spectrum shows the typical features expected for tubular J-aggregates with several sharp and red-shifted absorption bands. Morphological investigations using cryo-transmission electron microscopy (cryo-TEM) and spectroscopic investigations reveal a high stability of the tubular morphology but a tendency of the aggregates to assemble into ropelike bundles after several weeks of storage. It is found that aggregation in solutions containing additives such as alcohols or surfactants results in the formation of new types of aggregates. A second type of tubular aggregate with a diameter of 13.0 ± 0.5 nm is observed when the solutions contain more than 10 wt % MeOH. On the time scale of days these tubular aggregates transform into ribbonlike structures characterized by a new absorption spectrum, and they convert after several weeks into giant tubes with diameters of up to 500 nm.

I. Introduction

J-Aggregates of cyanine dyes are an exciting object of research since their discovery in the 1930s.[1,2] These aggregates are formed in polar solvents upon increasing the concentration above a critical level. The association of the cyanine dye molecules into mesoscopic aggregates is not only driven by the hydrophobic effect (solvophobic forces) but also particularly favored by strong attractive dispersion forces due to the high ground-state polarizability of the cyanine dyes.[3,4]

The most outstanding features of these aggregates are their peculiar optical properties. They are based on the exceptionally strong interaction between the transition dipole moments of the dye monomers. This leads to excitations that are extended over several molecules (excitons) and shifted in energy with respect to the monomer transition, as becomes evident from the optical absorption spectra. It is generally accepted that these excitonic spectra can be explained by Frenkel's model of molecular excitons,[5] which is based on dipole−dipole coupling between the transition dipole moments of neighboring molecules. Therefore, the optical properties of molecular aggregates strongly depend on the spatial arrangement of the dye molecules within the aggregate.[6,7]

Many peculiar linear and nonlinear optical properties of the aggregates result from the collective nature of excitations, namely, resonant fluorescence,[1,2] super radiant emission,[8−10] energy migration[11−14] and the related superquenching,[15] high nonlinear susceptibilities,[16] and efficient exciton−exciton annihilation.[17] Scientific interest in these properties stimulates fundamental research on molecular aggregates. Furthermore, efficient light energy harvesting and excellent transport capabilities make these aggregates promising candidates for artificial photosynthetic systems.[18,19] Synthesis of novel dye molecules that potentially lead to the formation of molecular aggregates with controlled morphology and, consequently, optical properties are of major importance.

Recently Dähne and co-workers developed a new family of amphiphilic cyanine dyes. These dyes consist of the well-known 5,5′,6,6′-tetrachlorobenzimidacarbocyanine chromophore[20] to which alkyl chains at the 1,1′ position of the nitrogen atoms and different acido- or sulfoalkyl substituents at the 3,3′ position (cf. Chart 1) have been attached. The length of the alkyl chains was selected in a range that is short enough (less than dodecyl) to maintain water solubility but is sufficient to stabilize the structures by hydrophobic interactions.

A large series of these dyes has been synthesized[21,22] and characterized.[23−26] It was found that competing molecular interactions led to a large variety of aggregate morphologies and structures. Furthermore, the appearance of J-aggregate spectra is a common feature of all of these structures. Because of the energy migration effects the dyes have been named "amphi-PIPEs" (*amphi*philes with *p*igment *i*nteraction *p*erforming *e*nergy migration).

Cryo-transmission electron microscopy (cryo-TEM) turned out to be an excellent technique to characterize the morphology of the amphi-PIPE aggregates. This technique was successfully and extensively applied to a selection of the amphi-PIPEs, namely, the carboxy-substituted types C8O3 and C8O4,[27−33]

* To whom correspondence should be addressed: e-mail berlepsc@chemie.fu-berlin.de.

† Freie Universität Berlin.

‡ Humboldt Universität zu Berlin.

§ University of Groningen.

|| Present address: Institut für Photonik, Technische Universität Wien, Gusshausstrasse 27/387, A-1040 Wien, Austria.

10.1021/jp065826n CCC: $37.00
Published on Web 01/30/2007

CHART 1: Principal Structure of Amphi-PIPE Molecules[a]

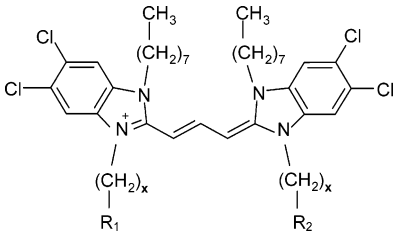

[a] For C8OX, X = 3, 4; $R_1 = COO^-$; $R_2 = COOH$. For C8SX: X = 2, 3; $R_1 = SO_3^-$; $R_2 = SO_3Na$.

and to the sulfo-substituted dyes C8S2[34] and C8S3.[35] The common feature of all aggregates is the packing of the dye molecules in a molecular bilayer arrangement.[27] This particular packing motif permits the hydrophobic (octyl) side chains to segregate from the surrounding aqueous medium. It was a surprising result that the bilayers of all amphi-PIPEs except for C8O4[30] can form tubular structures on the mesoscopic scale. The tubules are often assembled into helically twisted bundles. For example, the ropelike bundles of C8O3[27,32] consist of 5−10 tubules with a typical diameter of ∼10 nm each and extend in length to more than several hundreds of nanometers.

The 3,3′-bis(2-sulfopropyl)-5,5′,6,6′-tetrachloro-1,1′-dioctylbenzimidacarbocyanine dye (C8S3) differs from the comprehensively studied C8O3 derivative by the terminating side groups. Sulfo groups replace the carboxyl groups of the C8O3 derivative. In aqueous solution, C8S3 forms single and almost straight tubular aggregates with uniform diameter.[35] Bundling is largely absent and occurs only on time scales of several weeks or months.

Subsequent experiments revealed, however, a strong influence of the conditions of sample preparation on the optical properties of C8S3 aggregates. Thus, it became evident that different tubular aggregate structures are formed in aqueous solution when prepared either by direct dissolution of the crystalline material or by dilution from an alcoholic stock solution. Also, the presence of surfactants causes the formation of several new microstructures with novel optical properties. Similar effects were already known for the amphi-PIPE C8O3,[29,31,32] but they seem to be dramatic in case of C8S3. The structural changes have been traced back to the amphiphilic nature of the additives and the formation of mixed aggregates. In order to guarantee the reproducibility of further experiments, a systematic study of the effect of preparation conditions and of amphiphilic additives appeared quite important and was undertaken here. The main results are reported.

The paper is organized as follows: The formation of two different types of tubular J-aggregates, depending on the conditions of preparation, will be discussed in the first section (III.1). The optical and mesoscopic structural characteristics of both types of aggregates are separately discussed in more detail in the following two sections (III.2 and III.3). Here, the effect of surface-active additives is discussed. Moreover, it will be shown that the tubular aggregates are typically not in thermodynamic equilibrium but subjected to morphological transformations. The transformation of tubular J-aggregates into ribbons and later into giant tubes will be discussed separately in section III.4.

II. Experimental Section

Materials. Synthesis, purification, and analytical characterization of the C8S3 dye and other 5,5′,6,6′-tetrachlorobenzimidacarbocyanine derivatives are described in detail in ref 22. The dye C8S3 available as betain salt was supplied by FEW Chemicals (Wolfen, Germany) and was used as received. The molecular mass is 902.8 g/mol. The molar extinction coefficient in dimethyl sulfoxide (DMSO) (at $\lambda = 528$ nm) was found to be $\epsilon = 1.40 \times 10^5$ L/(mol·cm).[36] Sodium dodecyl sulfate (SDS) was synthesized and purified in our laboratory to a purity better than 99%. Methanol (99.9%, water <0.005%) was purchased from Fluka, and ethanol (p.a.) was from Merck. (*R*)- and (*S*)-2-octanol (total amount of enantiomers 99%) were obtained from Fluka. Due to their low water solubility, the chiral alcohols were first dissolved in ethanol (180×10^{-3} M) and then added to the solvent by using a microliter syringe (Hamilton). Double-distilled deionized water was used for preparation of the solutions.

Samples. C8S3 aggregates were prepared in two different ways. In the "direct route", the dye was dissolved in pure water as the solvent. Due to its poor water solubility, stirring for 1 week was necessary at room temperature. Stock solutions of $\sim 4 \times 10^{-4}$ M dye were thus obtained and diluted for spectroscopy, if necessary. Within the limits of experimental error (±10%), the absorbance of different stock solutions was reproducible. The second method of preparation is called the "alcoholic route". Here the dye was first completely dissolved in MeOH and then added to the solvent (commonly pure water) for aggregation. These mixtures were first vigorously shaken to become homogeneous and then stored without stirring in the dark for 24 h. The $\sim 4 \times 10^{-4}$ M dye solutions prepared as described are slightly opalescent. No hint of residual undissolved or precipitated dye material was observed. The content of MeOH was commonly on the order of 20 wt %.

Methods. Isotropic absorption spectra were measured with a Lambda 9 spectrophotometer (Perkin-Elmer), fluorescence spectra with a luminescence spectrometer LS 50B (Perkin-Elmer), and circular dichroism (CD) spectra with a J-715 spectropolarimeter (Jasco Corp.). Linear dichroism (LD) spectra were measured by aligning the aggregates in a streaming flow (optical path length 0.2 mm) of the liquid and monitoring the absorption for light polarized parallel and perpendicular to the flow direction.[33] Spectroscopic measurements were carried out at room temperature (21 ± 1 °C).

Cryo-TEM was performed with a Philips CM12 transmission electron microscope at 100 kV. Sample grids were plunged into liquid ethane at its melting point for vitrification and imaged at $T = -178$ °C. Details can be found in ref 34.

III. Results and Discussion

III.1. Two Types of Tubular J-Aggregates. In Figure 1 the absorption spectra of two samples, prepared via the direct route (panel a) and the alcoholic route (panel b), are presented. Common for both samples are the two bands I [$\lambda_{max} = 605$ nm (direct) and 600 nm (alcoholic)] and II [$\lambda_{max} = 593$ nm (direct) and 589 nm (alcoholic)] on the long-wavelength side of the spectrum. In addition, in the case of direct route preparation a third band can be discerned at 582 nm (III). Upon aggregation from methanolic dye stock in water (alcoholic route), five bands are found; that is, in addition to the most pronounced bands I and II, a shoulder at 581 nm (III) and two weak bands at around 572 (IV) and 559 nm (V) are found. The absorption spectrum of the monomers, as measured in DMSO, is shown for reference in Figure 1a by a dashed line. It shows the characteristic absorption maximum at 528 nm for the 5,5′,6,6′-tetrachlorobenzimidacarbocyanine chromophore. The entire spectrum is red-shifted compared to the monomer spectrum, which indicates

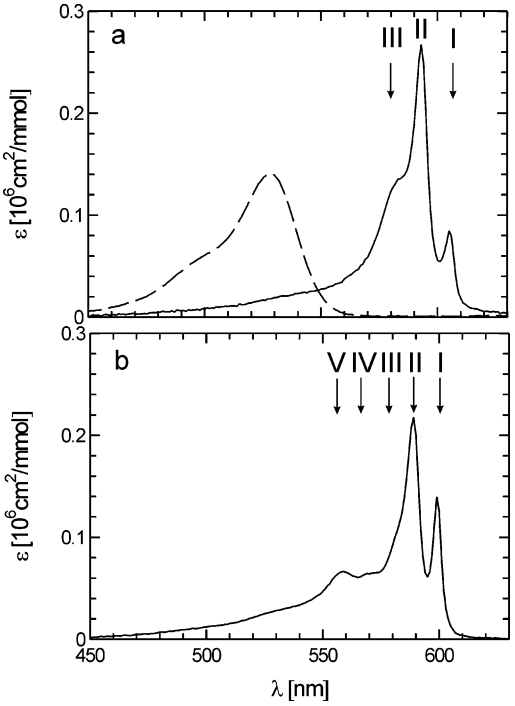

Figure 1. (a) Absorbance of a C8S3 solution (—) prepared via the direct route, measured after 7 days of stirring. [C8S3] = 3.4×10^{-4} M. The spectrum of C8S3 monomers in DMSO is added (— — —). (b) Absorbance of a 3.84×10^{-4} M C8S3 sample prepared via the alcoholic route from a methanolic stock solution. [MeOH] = 16 wt %. Shortly before the measurement, the 1-day-old stock solution was diluted with water (final dye concentration 6×10^{-5} M).

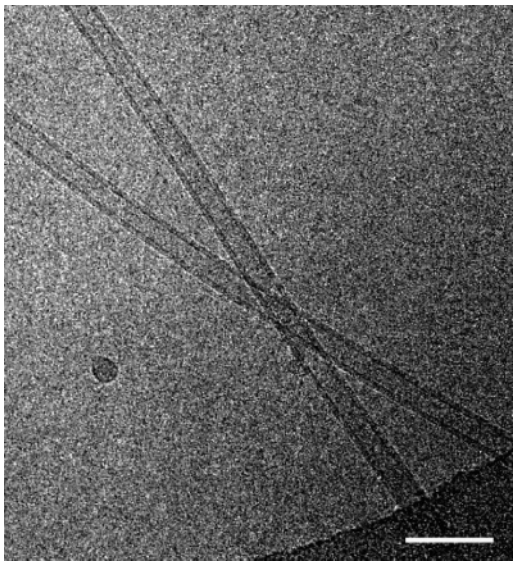

Figure 2. Cryo-TEM image of a 3.4×10^{-4} M C8S3 sample prepared via the direct route 9 days after preparation. The dark spot is due to surface contamination. Bar = 50 nm.

negative (J-type) interaction energy between the transition dipole moments of neighboring dye molecules. The appearance of structured spectra composed of several subbands is the typical signature of tubular aggregates of amphi-PIPE molecules.[27,33]

A representative cryo-TEM micrograph of a 9-day-old C8S3 solution prepared via the direct route in water is shown in Figure 2. The image shows two individual tubules, which are rather straight and typically several hundred nanometers long. The total diameter of these tubules is 17.0 ± 0.5 nm with a wall thickness of 4.0 ± 0.5 nm. The wall thickness is typical for packing of the dye molecules in a bilayer. The two constituting chromophore monolayers can be resolved at larger magnification.[35] Bundling of individual tubules has not been found for fresh solutions prepared via the direct route.

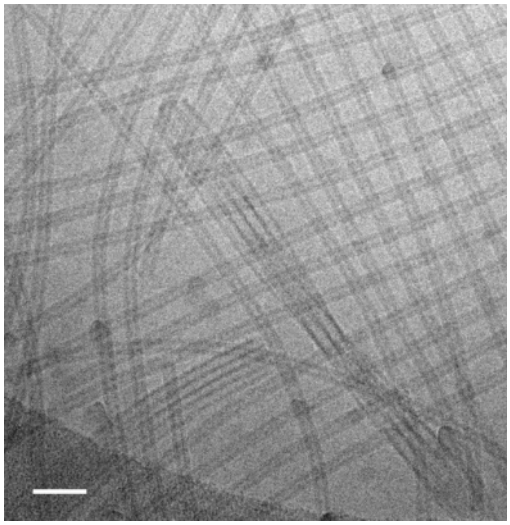

Figure 3. Cryo-TEM image of a 5.3×10^{-4} M C8S3 sample prepared via the alcoholic route 3 days after preparation. [MeOH] = 16 wt %. Bar = 50 nm.

A cryo-TEM micrograph of a C8S3 solution 3 days after preparation via the alcoholic route is shown in Figure 3. The image clearly reveals isolated tubular aggregates with uniform diameter of 13.0 ± 0.5 nm. Occasionally twisted or untwisted bundles of tubules can be detected. The wall thickness of the tubules is again 4.0 ± 0.5 nm (cf. Figure S1, Supporting Information).

The smaller tubule diameter in the case of the alcoholic route of preparation might be due to the increased flexibility of the bilayer upon incorporation of alcohol molecules.[37] Higher flexibility should allow for a higher curvature and hence a smaller cross-sectional diameter. A corresponding effect has not been observed for tubules of the C8O3 amphi-PIPE.[31] In this case the curvature of the tubules is extremely high (the tubule has a total diameter of about 10 nm and an inner channel of only ~2 nm) and a further increase in curvature is obviously not favorable.

III.2. Tubular J-Aggregates Prepared via the Direct Route. III.2.1. Spectroscopic Characterization. The occurrence of chirality, as detected by strong circular dichroism, is an outstanding feature of the tubular aggregates of the amphi-PIPEs previously investigated.[28] It has been shown for the C8O3 aggregates[38] that the chirality of the molecular packing (the molecule itself is achiral) predominates the CD spectrum. A nonracemic mixture of aggregates with one sense of helicity predominating explained the strong CD amplitude. Aggregate chirality is also found for the compound investigated here, as can be seen in Figure 4, where isotropic absorption (— — —) and CD (—) spectra of a 1.2×10^{-4} M solution prepared via the direct route are presented. The CD spectrum is characterized by three bands located at 570, 585, and 605 nm and having alternating signs (−, +, −). This spectrum is in surprisingly good agreement with the CD spectra recorded for the superhelical C8O3 J-aggregates[23,24,27,31] but with opposite sign of the amplitudes. Furthermore, good reproducibility of the CD signal in the present case is a strong indication that the spectra are governed by intrinsic chirality. However, the reversed sign of CD amplitudes with respect to the case of C8O3 aggregates[32] reveals that the prevailing handedness of helical arrangement of C8S3 molecules within the tubule is opposite.

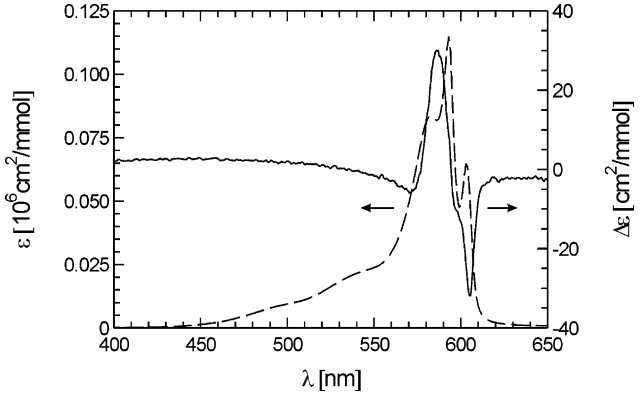

Figure 4. Absorption (− − −, left ordinate) and CD (—, right ordinate) spectra of a 1.2×10^{-4} M C8S3 solution 2 weeks after preparation via the direct route.

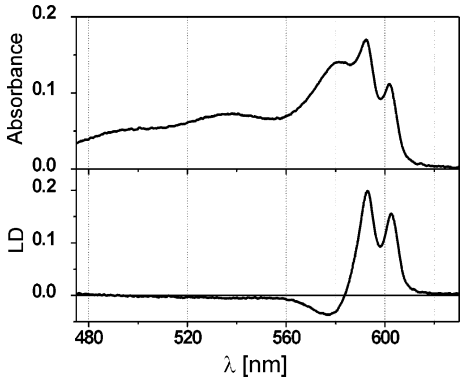

Figure 5. Isotropic absorption and LD spectra of a C8S3 solution 7 days after preparation via the direct route. [C8S3] = 3.4×10^{-4} M.

Polarized absorption spectra were measured on samples oriented in a streaming flow. The isotropic and linear dichroism spectra are compared in Figure 5. It is obvious that the two strong absorption bands (I and II) are governed by transitions with dipole moments oriented preferentially parallel to the axis of the aggregate, while in contrast, the third absorption band (III) represents transitions with favored perpendicular orientation.

The fluorescence spectrum of C8S3 aggregates shown in Figure 6 is a superposition of two bands that coincide with the absorption bands I and II and a shoulder at shorter wavelength. The excitation spectrum recorded at 605 nm is added (− − −). The relative intensity of the two main emission peaks differs from that of the absorption peaks and is independent of the excitation wavelength. The fact that the emission is in resonance with the absorption is typical behavior of J-aggregates. According to the Kasha rule, it is expected that any excitation into the exciton band will relax very fast into the level of lowest energy. The occurrence of the two fluorescence bands indicates that the fluorescence spectrum is governed by two weakly coupled excitons.[35]

Knoester and co-workers[25,26] proposed the first theoretical description of the absorption spectra using a model of cylindrical aggregates. Further improvement was made by Didraga et al.[35] by taking the double-layer wall structure into account. The aggregates were described by two tubes of slightly different diameter that fit into each other. Each tube is formed by rolling up a brickwork-like two-dimensional lattice of dye molecules. This model results in two exciton transitions for each of the tubes, both red-shifted with respect to the monomer absorption, with one polarized along the cylinder axis and the second one polarized perpendicular. Hence, the full spectrum of the aggregate consists of four transitions. This model gives excellent qualitative and quantitative agreement between the measured and calculated absorption and linear dichroism spectra[35] and also explains the observed steady-state and time-resolved fluorescence spectra.[39]

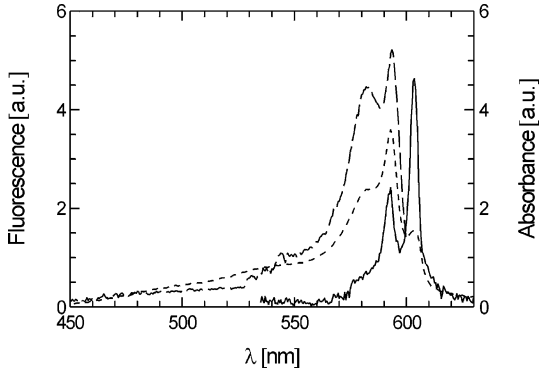

Figure 6. Absorption (right ordinate;---), fluorescence excitation (left ordinate; − − −) and emission spectra (left ordinate; —) of a C8S3 solution ([C8S3] = 2.75×10^{-4} M) 5 days after preparation via the direct route. For the fluorescence measurements the solution was strongly diluted ([C8S3] = 2.9×10^{-7} M, optical density OD (592 nm) = 0.04). The effect of reabsorption on the emission spectrum has been neglected. The excitation spectrum was collected at 605 nm; the emission spectrum was collected after excitation at 530 nm. The slit width of excitation and emission monochromators was set to 2.5 nm.

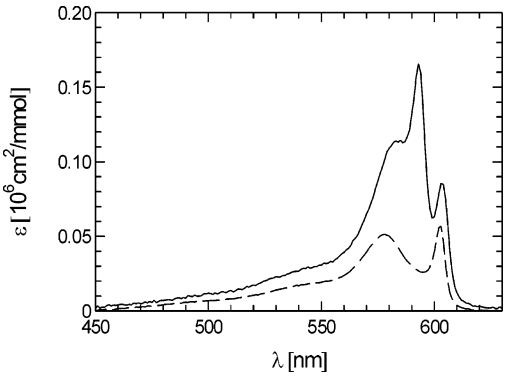

Figure 7. Absorbance of a 3.7×10^{-4} M C8S3 solution after preparation via the direct route (—) and after 5 months of storage (− − −).

III.2.2. Bundling of Tubules. All experiments described so far have been performed with freshly prepared solutions, that is, solutions not older than 2 weeks. However, observation of structural transformations in the case of C8S2 aggregates during storage over weeks and months[34] prompted us to look for similar instabilities in the case of C8S3.

Absorption spectra of a solution measured directly after preparation and after 5 months of storage in the dark are shown in Figure 7. Over this period of time a distinct bleaching of the total absorbance occurred and the originally three-banded spectrum transformed into a two-banded absorption spectrum. An analogous spectral transformation, that is, from a three-banded to a two-banded spectrum, has been induced by adding alcohols to aggregated C8O3 solutions. The spectral changes were ascribed to a modification of the molecular packing due to the incorporation of alcohol molecules.[31] In the present case the reason for the spectroscopic and hence structural changes is unclear, because special guest molecules have not been added. The bleaching of the total absorbance during storage might be due to a partial oxidation of the C8S3 molecule in aqueous medium.

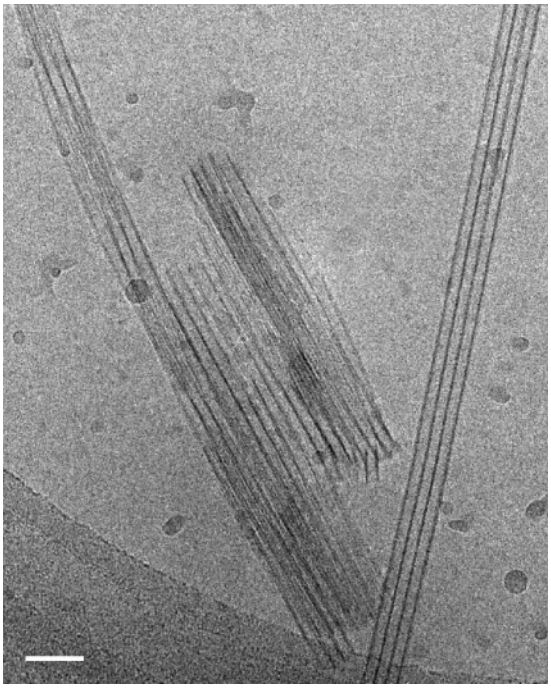

Figure 8. Cryo-TEM image of a 3.7×10^{-4} M C8S3 solution prepared via the direct route after 5 months of storage. Bar = 50 nm.

The aggregates' morphology of a 5-month-old solution of C8S3 exhibits a surprising similarity to those of C8O3 solutions containing alcohol. Figure 8 shows a cryo-TEM micrograph of the matured C8S3 solution. Only bundles (or fragments of bundles) of tubular aggregates are visible while isolated tubules were not detected, as in the case of the C8O3 aggregates after the addition of alcohols.[31] Thus, besides the analogous spectral behavior we find a similarity in the mesoscopic architecture of both types of aggregates.

The tendency of tubules to agglomerate into bundles has to be explained by attractive forces. In contrast to the carboxypropyl derivative C8O3,[31] stabilization by hydrogen bonding can be excluded for the sulfopropyl-substituted derivative C8S3. Due to the extended π-electron systems, however, dye assemblies are highly polarizable even in the ground state and thus are subject to attractive van der Waals forces. At short distances these forces may dominate and overcompensate the repulsive electrostatic forces.

III.2.3. Effect of Additives. Surfactants. The titration of aqueous C8S3 solutions (direct route) with the anionic surfactant SDS induces changes in the absorbance. Thus, with increasing SDS concentration the typical 3-fold split absorption spectrum becomes replaced (at a molar SDS/C8S3 mixing ratio of 15) by a 2-fold split spectrum (Figure S2, Supporting Information), comparable with that measured after long-time storage in the absence of SDS (Figure 7). During titration, obviously more and more surfactant molecules were incorporated into the aggregates, which disturbs their original packing structure and results in the new spectrum.[40]

In contrast to the anionic SDS, the addition of cationic surfactants [for example, trimethyltetradecylammonium bromide (TTAB)] leads immediately to precipitation. Such behavior is commonly observed when oppositely charged amphi-PIPEs and surfactant molecules are mixed and can be understood as the result of a highly cooperative ionic self-assembly process.[41]

Characterization of the C8S3−SDS system by cryo-TEM revealed two different morphologies. The predominant architecture is a ropelike superhelical aggregate (Figure S3a, Supporting Information). The similarity of the structural motif to that of the aged SDS-free sample (Figure 8) is evident. Although both host and guest molecules are equally charged (both are anionic), strong bundling had occurred. Van der Waals forces might again be responsible for the agglomeration. In order to reduce the strong electrostatic repulsion between the tubules, the counterions are obviously incorporated into the hydration layers. As a second morphology we found unilamellar vesicles with a typical diameter of ~20 nm (Figure S3b, Supporting Information). It is surprising that the common building principle of the J-aggregates, that is, the self-assembly of molecules into linear objects, seems to fail here. Possibly the fraction of incorporated surfactant molecules is much larger in unilamellar vesicles than in the cylindrical aggregates, what could allow for a higher curvature of the bilayer and the formation of small spherical particles.

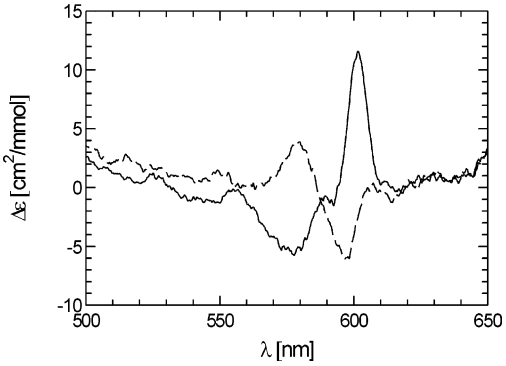

Figure 9. CD spectra of two 3.55×10^{-5} M C8S3 solutions prepared via the direct route to which *R*-(2)-octanol (—) or *S*-(2)-octanol (— — —) was added after aggregation. One day was waited for equilibration between addition of chiral alcohol and CD measurement. [EtOH] 3 wt %; molar mixing ratio [octanol]/[dye] = 34.

Chiral Alcohols. Alcohols are weak amphiphiles. After addition, they preferentially occupy regions at the surface of the aggregates and influence the packing of dye molecules by partitioning between them. Recent studies have shown[32] that the helicity of the C8O3 J-aggregates can be controlled by chiral alcohols. Upon addition of respective enantiomerically pure alkanols, the CD signal was enhanced by a factor of at least 100 and even reversed. Moreover, it was observed that the handedness of the helical superstructure and the CD signature are correlated. Because the sulfonated derivative C8S3 shows optical activity as well, we anticipated similar behavior here.

Indeed, the CD spectrum of a pure C8S3 solution (cf. Figure 4) exhibits the same signature (−, +, −) as C8O3 solutions aggregated in the presence of (*S*)-2-octanol.[32] Therefore, it could be expected that the addition of (*S*)-2-octanol to a pure C8S3 solution should at most amplify the CD signal but not change its signature. After addition of the alcohol and equilibration of the sample for 1 day, the CD spectrum did not show a change in the CD signature, though amplification effects were also absent (Figure 9, — — —). Adding (*R*)-2-octanol to a second C8S3 sample reversed the signature as expected, while the strength of the CD signal was again not enhanced (solid line in Figure 9). The reversal of the signal proves a kind of induced chirality in agreement with the older C8O3 experiments, however with a much smaller net effect. Accompanying absorption measurements did not reveal qualitative changes in the shape of the spectra, and the CD signal cannot be related to any new structural effect observable by cryo-TEM.

MeOH. Given their amphiphilic nature, short-chain alcohols primarily confine themselves to the hydrophilic headgroup region of the aggregated chromophores instead of the hydro-

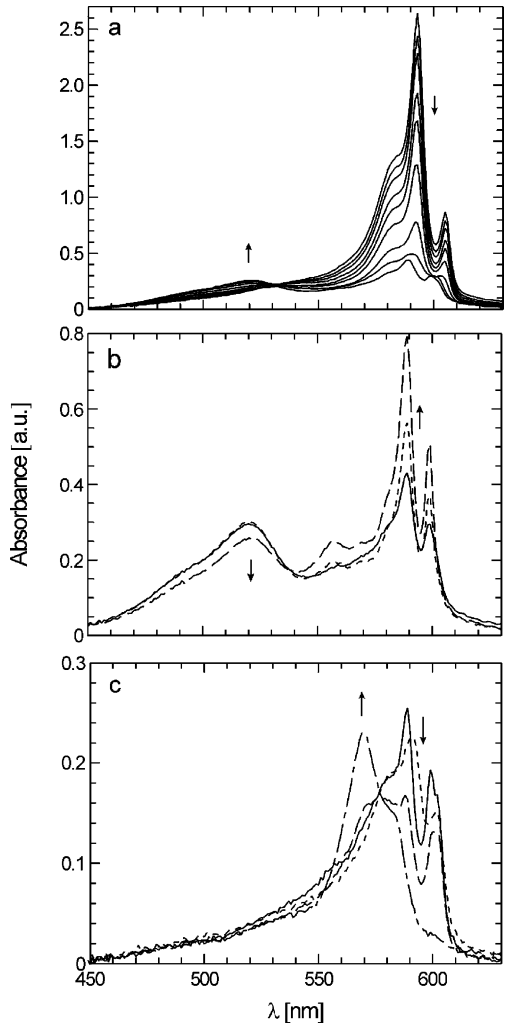

Figure 10. (a) Change of absorption spectra of an 1.45×10^{-4} M C8S3 solution prepared via the direct route as a function of added MeOH. [MeOH] (in weight percent): 0, 2.75, 5.5, 8.25, 11.0, 13.75, 16.5, 19.25, and 22.0. Arrows indicate the effect of increasing MeOH concentration. (b) Temporal evolution of absorbance after the addition of 25 wt % MeOH. Arrows indicate increasing time (in minutes) after addition: 1 (—), 30 (---), and 45 (— — —). (c) Long-time changes in the absorbance of a 3.4×10^{-4} M C8S3 solution prepared via the direct route after the addition of 16 wt % methanol. Arrows indicate increasing time after addition: 1 min (—), 1 day (---), 2 days (— — —), and 6 days (— - —).

carbon core of aggregates.[37] Thereby they affect the spatial arrangement of chromophores and their optical properties. This became evident during the sample preparation (section III.1), when two different types of tubular aggregates evolved depending on the presence or absence of MeOH. This finding makes MeOH a special additive justifying more detailed investigations.

We first studied the effect of MeOH by absorption spectroscopy. The set of curves plotted in Figure 10a was obtained from a C8S3 solution prepared in pure water by titrating with MeOH. The holding time between each titration step was 3 min. Up to [MeOH] ~18 wt %, the absorbance in the long-wavelength region (bands I−III) strongly decreased while the shape of the spectrum remained almost unaffected. Above this critical MeOH concentration, bands I−III shift to the blue side with the maxima now located at 600 nm (I), 589 nm (II), and 581 nm (III), which values exactly correspond to those positions obtained from the alcoholic route of preparation (cf. Figure 1b).

It is remarkable that only these two distinct types of aggregates are observed and no intermediate structures were found. The changes on the red side of the absorption spectrum are accompanied by an increasing monomer band (peak at ~520 nm) with an isosbestic point at around 530 nm. Over all, the spectroscopic pattern indicates a progressive dissolution of J-aggregates into monomers with increasing MeOH content and a transformation of the type of tubular J-aggregate into another one above a threshold concentration of about 18 wt %. However, as will be shown in the next section, this value also depends on kinetic factors.

III.2.4. Methanol-Induced Structural Transformations. It is a general feature of all MeOH-containing aggregated solutions that they undergo structural transitions with time, where the relevant time scales can range from minutes to days, weeks, and even months. In this section we consider the case where MeOH is added to aggregated solutions prepared in pure water, while the samples prepared via the alcoholic route will be discussed separately in sections III.3 and III.4.

First we consider the time domain up to 1 h. Figure 10b shows the time evolution of the absorbance after addition of MeOH (25 wt %) into a solution of aggregates in pure water. Immediately after the addition a spectrum was recorded that fits quite well into the set of curves displayed in Figure 10a (here the maximum MeOH content was 22 wt %). Within 45 min all five bands characteristic for samples prepared via the alcoholic route evolved. At the same time the monomer band became weaker but still remains due to the large amount of MeOH present in the solvent.

To monitor the changes occurring within the time domain from 1 h to 1 week, we started again with a pure aqueous solution of aggregates but added a smaller amount of MeOH (only 16 wt %) to slow down the kinetics. The absorption spectra plotted in Figure 10c were measured immediately after addition as well as after 1, 2, and 6 days of storage. Apart from a slightly decreased overall intensity due to the dilution, MeOH did not show any effect on the shape of the spectrum immediately after addition, which is in accordance with the earlier titration experiment (Figure 10a). After 1 day of storage, however, changes in the spectral shape became visible. Bands I and II became weaker and shifted toward longer wavelengths, while the absorbance in the vicinity of band III remained largely unaffected. After 6 days of storage a quite new spectrum has emerged, characterized by the disappearance of bands I and II, a strong and wide band at ~570 nm, and an additional shoulder at around 583 nm. The drastic change in the absorption spectrum indicates a transformation from the tubular morphology into a new structure (cf. section III.3.2, Figures 12 and 13). Lengthening the storage time up to several weeks did not produce further spectral changes.

III.3. Tubular J-aggregates Prepared via the Alcoholic Route. The tubular aggregates investigated in this chapter were prepared exclusively via the alcoholic route, that is, the dye was first completely dissolved in MeOH and then added into water for aggregation. The MeOH concentration was typically in the range of 10−25 wt %.

III.3.1. Spectroscopic Characterization of Tubules. The isotropic absorption spectrum of a typical sample prepared via the alcoholic route (already shown in Figure 1b) consists of five bands within the 550−610 nm wavelength range and a tail toward smaller wavelengths.

In contrast to the alcohol-free samples, which have well-defined and reproducible CD spectra (cf. Figure 4), the samples prepared via the alcoholic route gave usually nonreproducible

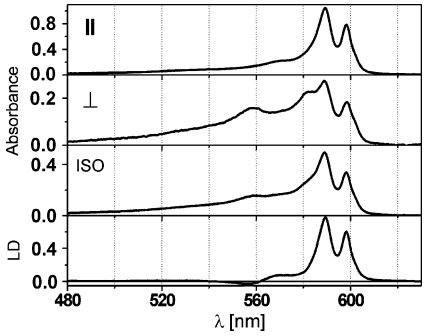

Figure 11. Isotropic absorption spectrum (ISO) and absorption spectra measured for light polarized parallel (∥) and perpendicular (⊥) to the flow direction of a C8S3 solution prepared by the alcoholic route. The LD spectrum was calculated from the dichroic absorption spectra. Sample [C8S3] = 2.35×10^{-4} M; [MeOH] = 20 wt %; measurement 1 h after sample preparation.

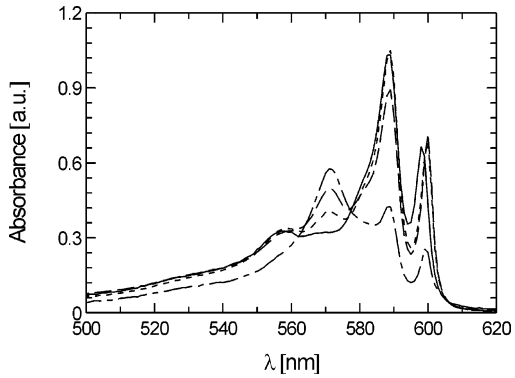

Figure 12. Storage time dependence of the absorbance of a 4.2×10^{-4} M C8S3 solution prepared via the alcoholic route. The initial MeOH concentration was 19.5 wt %. For the measurement the sample was diluted with water down to 3.6×10^{-5} M. Storage time after preparation: 10 min (—), 1 day (---), 2 days (— — —), and 17 days (— - —).

signals that point to large contributions from linear dichroism.[42] The small contribution from intrinsic chirality to the total CD signal does not necessarily disprove the chirality of tubules but only indicates that both senses of handedness occur with nearly equal probability. In this respect, the MeOH-containing C8S3 aggregates differ from those prepared in the absence of MeOH and especially from the C8O3 aggregates, which form nonracemic mixtures with a specific sense of handedness predominating.[31,32]

Polarized absorption spectra on flow-oriented aggregates are shown in Figure 11. The isotropic solution is characterized by the 5-fold absorption spectrum. Despite a small blue shift by approximately 2 nm, the two outmost red absorption bands (I and II) remain practically unchanged compared to pure C8S3 aggregates (Figure 5). In contrast, the situation in the spectral range of 550−580 nm changes dramatically. The absorption band centered at ∼581 nm (III), representing the perpendicularly oriented transition in the absence of MeOH, decreases in intensity. Instead, new absorption bands at around 570 and 555 nm are found for parallel polarized light. The absorption on the blue side of the spectrum appears to be isotropic and unaffected by the presence of MeOH. The LD spectrum shows only two positive bands and one negative band, as in the MeOH-free case, but now at different wavelength positions.

The fluorescence spectrum of MeOH-containing solutions (Figure S4, Supporting Information) is quite similar to the spectrum in the absence of MeOH (Figure 6). In each case the spectrum is composed of two bands that coincide with the respective absorption bands I and II.

III.3.2. Tubular and Ribbonlike Aggregates Coexist. Figure 12 shows the evolution of the absorbance as a function of time after preparation of a sample with a methanol content of 19.5 wt %. Within 17 days a new band forms at around 570 nm at the expense of a substantially reduced intensity of bands I−III. Also, band V is reduced but still visible as a shoulder even after 17 days. The new 570 nm band does not coincide with band IV of the tubular aggregates, but is the same band as already discussed above for another preparation (Figure 10c). It indicates a novel species.

Figure 13 shows a representative cryo-TEM micrograph of the 17-day-old sample of Figure 12. One finds a coexistence of isolated tubules, twisted bundles of tubules, and ribbonlike aggregates (marked by asterisks). The ribbonlike structures have not been observed before and are considered a new type of aggregate. The typical width of the ribbons is about 30 nm. The thickness can be estimated from the parts of ribbons oriented on edge in the embedding ice. A value of 3.8 ± 0.2 nm is obtained and confirms the suspected tail-to-tail bilayer organization of the dye molecules.[27]

A coexistence of tubular and ribbonlike J-aggregates was previously observed for the dye C8S2 when small amounts of MeOH were present.[34] As in the present case, the tubular aggregates became unstable on time scales of weeks and converted into ribbons. In contrast to the aggregates of C8S2,

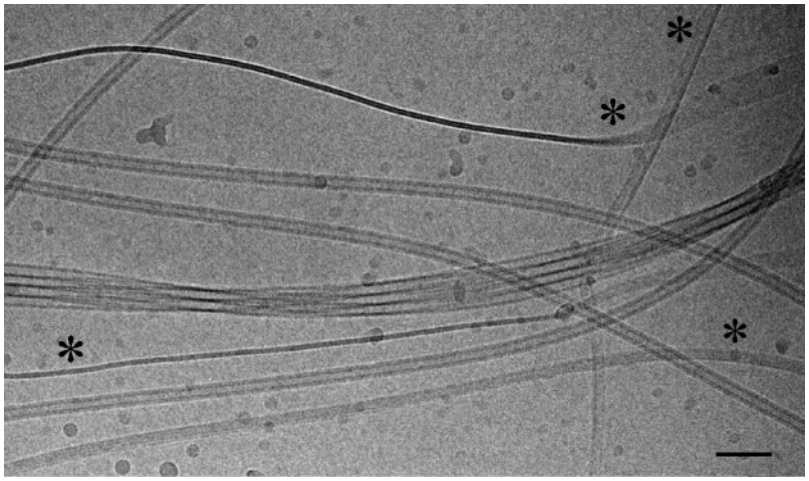

Figure 13. Cryo-TEM image of a 4.2×10^{-4} M C8S3 solution prepared via the alcoholic route after 17 days of storage (cf. Figure 12 for the absorption spectrum). Isolated tubules, a twisted bundle of tubules, and bilayered ribbons (indicated by asterisks) coexist. Bar = 50 nm.

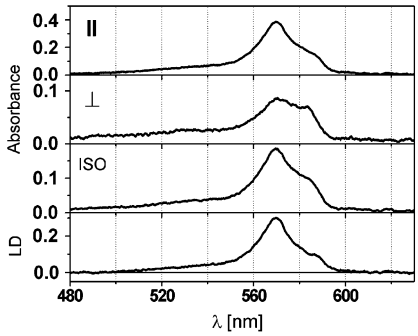

Figure 14. Isotropic absorption spectrum (ISO) and absorption spectra measured for light polarized parallel (∥) and perpendicular (⊥) to the flow direction of a C8S3 solution with ribbon-like aggregates. The LD spectrum was calculated from the dichroic absorption spectra. The sample was the same as used for Figure 11 but after the tubules were converted into ribbons within 2 days of stirring. [C8S3] = 2.35×10^{-4} M; [MeOH] = 20 wt %.

where the ribbons are generally assembled into multiple stacks,[34] the ribbons of C8S3 show a low tendency to stacking. The slow rate of structural transformation can be explained by the multiplicity of molecular interactions involved.[43] Additionally, one should note that the dye molecules forming the J-aggregates are tied up by reversible linkages, which may undergo assembly and disassembly in response to external factors. We assume that the transformation from tubular to ribbonlike structures is governed by two competing terms of the free energy of the system, namely, the bending energy of the dye−bilayer membrane on one hand and the edge energy of the layers on the other hand. Tubular aggregates are stable structures that are characterized by a finite bending energy at the expense of a vanishing edge energy. Decreasing the specific edge energy, for example by adding alcohol, should favor planar structures with exposed edges, that is, ribbons. Because the cost in energy for breaking the tubular organization is obviously very high, a slow rate of transformation is observed. Interestingly, the aggregates of the dye C8O3 retain their tubular structure upon addition of MeOH.[31] Here the increased stability might be explained by additional stabilizing hydrogen bonds between the carboxyl groups.

III.4. Tubule-to-Ribbon-to-Tube Transition. In the preceding section we have shown that the dye C8S3 can form ribbonlike J-aggregates in addition to tubular ones when MeOH is present. The involved phenomenology of the process by which tubules transform into ribbons necessitated more detailed investigations. Long-time studies were unavoidable because the observed coexistence of both types of aggregates indicated that the transformation was probably not completed on the time scale of several days. Else, it had to be checked if there were further experimental parameters that control the structural transformation.

III.4.1. Preparation and Characterization of Ribbonlike J-Aggregates. Looking for the parameters suspected to trigger the transformation of tubules into ribbons, we first varied the concentration of MeOH.

Interestingly, we found that a solution prepared via the alcoholic route containing only 10 wt % MeOH behaved like an alcohol-free solution. Even after 1 year of storage the 570 nm peak characteristic for the ribbons did not appear, while instead two bands centered at around 605 and 575 nm were measured (Figure S5, Supporting Information). This type of spectrum is typical for bundles of tubular aggregates (cf. Figure 7); that is, ribbonlike aggregates did not form.

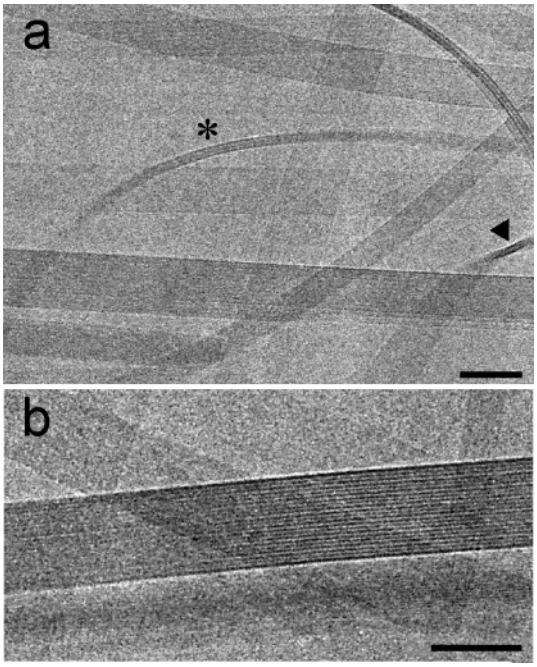

Figure 15. Cryo-TEM images of a 5.6×10^{-4} M C8S3 solution, which has been stirred for 1 day after preparation via the alcoholic route (24 wt % MeOH) and then stored for 3 months. Only ribbonlike aggregates of bilayer (▼) or double-bilayer thickness (∗) are seen (panel a). Some ribbons show a distinct pattern of fine lines (panel b). Bar = 50 nm.

In a second experiment we added additional MeOH (up to a total concentration of 39 wt %) to a solution of tubules prepared via the alcoholic route. Fast titration of MeOH caused disaggregation (Figure S6, Supporting Information) but did not enhance the formation of ribbonlike aggregates.

Next we investigated the effect of stirring. We observed that the formation of ribbons was remarkably accelerated when the solutions were stirred (by use of a magnetic stirrer, 5 mm Teflon stir bars, and stirrer speeds of ∼250 rpm). The tubular aggregates of fresh solutions, which contained 20−25 wt % MeOH, could thus be completely transformed into ribbons (checked by cryo-TEM) within 1 day of stirring. Obviously, the small input of mechanical energy helped to reduce the kinetic barrier.

Figure 14 shows the isotropic spectrum and polarized absorption spectra, measured in a flow cell, of a sample with 20 wt % MeOH and after 2 days of stirring. The spectrum is characterized by two transitions at ∼570 and 583 nm, whereas the 570 nm band generally dominates the absorption spectrum. Although the measurements do not show complete polarization, one can deduce that the main transition is polarized parallel to the long axis of the aggregates, while the shoulder at 583 nm is polarized perpendicular. At present it is not clear if the two transitions belong to one molecular structure, or if there are two species with different preferential orientation of the molecules relative to the aggregate axis. A sometimes observed dependence of relative strength of transitions on the conditions of sample preparation (an example is shown in Figure S7, Supporting Information) rather points to different species. A contribution from residual tubules can almost certainly be excluded, because this would yield additional absorption bands at longer wavelengths (cf. Figure 12).

The morphology of the aggregates was thoroughly characterized by cryo-TEM. While tubules were still visible for the unstirred 17-day-old sample (Figure 13), they have completely disappeared after stirring and/or long-time aging. Solely rib-

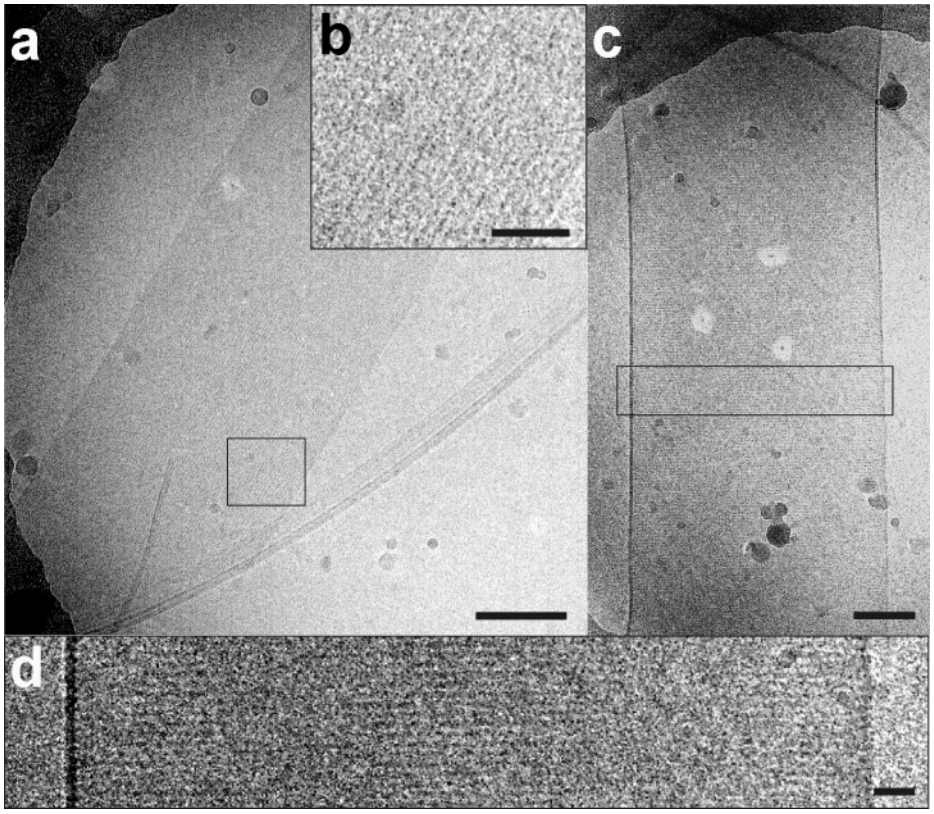

Figure 16. Cryo-TEM images of a 5.4×10^{-4} M C8S3 solution prepared via the alcoholic route (25 wt % MeOH) after 7 months of storage. (a) Low-magnification image showing a flat ribbon of ~300 nm width; bar = 100 nm. (b) The boxed region reveals a pattern of fine lines at high magnification (bar = 20 nm), oriented parallel to the long axis of the ribbon. (c) Low-magnification image showing a ~400 nm wide tubular aggregate; bar = 100 nm. (d) High magnification reveals a pattern of lines, oriented perpendicular to the aggregate axis. Bar = 20 nm.

bonlike aggregates are visible, as shown in the representative micrographs of Figure 15. In this case the solution was 3 months old and the 570 nm band dominated the respective absorption spectrum. No spectral features were observed that are indicative for residual tubules. The morphology of the ribbons appears to be rather uniform. Their average width increased with aging and reached typical values of 50 nm (as compared to 30 nm in Figure 13). But more striking is the growth in thickness. The aggregates marked by a triangle and an asterisk in Figure 15a have thicknesses of 3.8 ± 0.2 and 6.9 ± 0.2 nm, respectively, which corresponds to a single or a doubled bilayer. Stacks of more than two bilayers have not been observed.

Due to the stacking of two bilayers, the contrast of the cryo-TEM images is enhanced, which reveals a marked fine structure within the aggregates. A pattern of lines is often seen that is oriented parallel to the long axis of ribbons, cf. for example Figure 15b. The spacing of lines of 2.3 ± 0.2 nm ranges between the length of a molecule of about 2 nm and the typical stacking distances (bilayer thickness). The pattern is not a direct view of the molecular architecture but, nevertheless, seems to originate from a highly ordered molecular packing of the chromophores or related interference effects (moiré pattern). A comparable line motif has also been reported for the ribbonlike C8O4[27] and C8S2[34] aggregates.

III.4.2. "Dissolution" of Ribbons and Reassembly into Giant Tubes. The morphological investigations on ribbonlike aggregates reported so far revealed only a slight tendency of the individual aggregates to form stacks. This contrasts with former investigations on the C8O4 and C8S2 aggregates, where stacking of many individual ribbons into fibrillar assemblies was found regularly. The idea that stacking might be limited solely by very slow kinetics inspired the investigation of C8S3 solutions that were stored for several months.

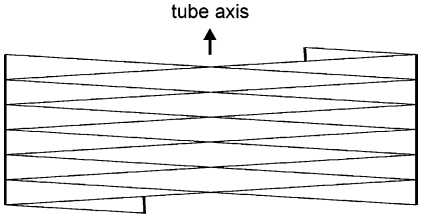

Figure 17. Schematic representation showing formation of the line pattern observed by cryo-TEM (Figure 16d). The helical marking has been exaggerated for clarity.

A sample, which was investigated after 7 months of storage, showed again the typical absorption spectrum governed by a strong band at 570 nm with a shoulder at 583 nm; that is, novel species are not indicated. Cryo-TEM micrographs are presented in Figure 16. Stacks composed of more than two bilayers were not found; however, the width of ribbons has dramatically increased. Typical values now range between 300 and 500 nm (panel a), which is by a factor of ~10 larger compared to the sample investigated after 3 months of storage (Figure 15). At larger magnification (panel b), the periodic stripe pattern oriented parallel to the long axis of the aggregates with a spacing of ~3.5 nm can also be detected. The structural motif seems unaffected.

On closer examination of the cryo-TEM images, however, a new morphology can be identified. Elongated objects of higher contrast compared to the flat ribbons are found (panel c) with a width on the order of 400−500 nm and a length in the range of 1 μm. Again a stripe pattern can be detected, but it is oriented perpendicularly to the long axis of these aggregates (panel d). Close inspection of these stripes reveals a moiré pattern as it occurs from the superposition of two stripe patterns tilted against each other. Such a pattern is expected when a longitudinally

striped ribbon is helically wrapped into a cylinder; cf. the scheme in Figure 17. The helical pitch is only 2 times the width of stripes, that is, about 7 nm. Therefore, it is assumed that these new objects represent giant tubes.

The formation of the giant tubes can qualitatively be explained by the following argumentation, which was given earlier in the context of the transformation of tubules into ribbons.[43] The driving force is the competition between the free energy gain from the face-to-face attraction between bilayers and the penalty due to the edge energy. When stacking of ribbons is favorable, such as in the case of the C8O4 and C8S2 aggregates, large edge energy can be tolerated. For C8S3 aggregates, stacking seems most unfavorable and the edge energy promotes growth of ribbons in length and width. Yet closure into tubes can further minimize the total free energy. The required bending energy is gained from the suppression of the high-energetic ribbon rims. The obvious high bending rigidity of ribbons results in relatively large tube diameters. The observed small helical pitch can be considered as an indication that the conversion of flat ribbons into giant tubes needs "dissolution" and reconstruction of the aggregates, but it cannot by obtained by helical wrapping of preformed ribbons. However, intermediate states, which could help to clarify the process of transformation, have not been detected so far.

IV. Conclusions

Addition of alcohols and surfactants to aggregated solutions of the amphiphilic tetrachlorobenzimidacarbocyanine dye C8S3 leads to the formation of mixed J-aggregates, which dramatically differ with respect to their morphological structure and the related optical properties from the original aggregates.

The effect of MeOH on aggregation was studied in detail. It was found that, for aqueous solutions with MeOH concentrations up to about 10 wt %, tubular aggregates with a diameter of 17.0 ± 0.5 nm are formed that are stable over time. They tend to form only bundles. At higher MeOH concentrations the tubules are reduced in diameter (13.0 ± 0.5 nm) and become unstable with time. On the time scale of several days and weeks they transform into ribbonlike structures. This MeOH-induced tubule-to-ribbon transition resembles a similar one previously reported for the dye C8S2. However, the ribbons show strikingly different stacking behavior. In the case of C8S2 they self-assemble into fibrillar assemblies, while they prefer to remain isolated bilayer ribbons or double at the most in the case of C8S3. On long time scales of months, the ribbons convert into giant tubes. The time dependence proves that, in general, the observed structures are not in thermodynamic equilibrium but instead are long-lived metastable states.

Although the aggregates formed in water/MeOH mixtures are subject to changes with time, the dynamics is slow enough to allow reproducible investigations of the aggregates by various methods, such as optical spectroscopy or cryo-TEM imaging. The outstanding regularity of the tubular structure and the clear structure of the absorption spectrum makes them favorable candidates for further investigations of the specific optical properties of J-aggregates in solution.

Acknowledgment. We thank Professor S. Dähne for kindly providing a sample of the C8S3 dye. The CD spectra were measured at the MPI für Kolloid- und Grenzflächenforschung, which is gratefully acknowledged. H.v.B., S.K., and C.B. thank the Deutsche Forschungsgemeinschaft (SFB 448, Mesoskopisch strukturierte Verbundsysteme) for financial support. A.P. and R.H. acknowledge Nederlandse Organisatie voor Wetenschappelijk onderzoek (NWO) for financial support.

Supporting Information Available: Cryo-TEM image of a sample prepared via the alcoholic route at high magnification (Figure S1), absorption spectra after the addition of SDS (Figure S2) and cryo-TEM images of respective aggregates (Figure S3), emission spectrum of solution prepared via the alcoholic route (Figure S4), and absorption spectra as a function of MeOH content (Figure S6) and storage time (Figures S5 and S7). This material is available free of charge via the Internet at http://pubs.acs.org.

References and Notes

(1) Scheibe, G. *Angew. Chem.* **1937**, *50*, 51.

(2) Jelly, E. E. *Nature* **1936**, *138*, 1009.

(3) Dähne, S. *Z. Wiss. Photogr., Photophys. Photochem.* **1965**, *59*, 113.

(4) Maiti, P. K.; Lansac, Y.; Glaser, M. A.; Clark, N. A. *Liq. Cryst.* **2002**, *29*, 619.

(5) Davydov, A. S. *Theory of Molecular Excitons*; Plenum Press: New York, 1971.

(6) Czikkely, V.; Försterling, H. D.; Kuhn, H. *Chem. Phys. Lett.* **1970**, *6*, 207.

(7) Knoester, J. *J. Chem. Phys.* **1993**, *99*, 8466.

(8) de Boer, S.; Vink, K. J.; Wiersma, D. A. *Chem. Phys. Lett.* **1987**, *137*, 99.

(9) Spano, F. C.; Mukamel, S. *J. Chem. Phys.* **1989**, *91*, 683.

(10) Meinardi, F.; Cerminara, M.; Sassella, A.; Bonifacio, R.; Tubino, R. *Phys. Rev. Lett.* **2003**, *91*, 247401.

(11) Sundström, V.; Gillbro, T.; Gardonas, R. A.; Piskarskas, A. *J. Chem. Phys.* **1988**, *89*, 2754.

(12) Moll, J.; Dähne, S.; Durrant, J. R.; Wiersma, D. A. *J. Chem. Phys.* **1995**, *102*, 6362.

(13) Scheblykin, I. G.; Sliusarenko, O. Y.; Lepnev, L. S.; Vitukhnovsky, A. G.; van der Auweraer, M. *J. Phys. Chem. B* **2000**, *104*, 10949.

(14) Ohta, K.; Yang, M.; Fleming, G. R. *J. Chem. Phys.* **2001**, *115*, 7609.

(15) Jones, R. M.; Lu, L.; Helgeson, R.; Bergstedt, T. S.; McBranch, D. W.; Whitten, D. G. *Proc. Natl. Acad. Sci. U.S.A.* **2001**, *98*, 14769.

(16) *J-Aggregates*; Kobayashi, T., Ed.; World Scientific: Singapore, 1996.

(17) Moll, J.; Harrison, W. J.; Brumbaugh, D. V.; Muenter, A. A. *J. Phys. Chem. A* **2000**, *104*, 8847.

(18) McDermott, G.; Prince, S. M.; Freer, A. A.; Hawthornthwaite-Lawless, A. M.; Papiz, M. Z.; Cogdell, R. J.; Isaacs, N. W. *Nature* **1995**, *374*, 517.

(19) van Amerongen, H.; Valkunas, L.; van Grondelle, R. *Photosynthetic Excitons*; World Scientific: Singapore, 2000.

(20) Herz, A. H. *Photogr. Sci. Eng.* **1974**, *18*, 323.

(21) De Rossi, U.; Moll, J.; Spieles, M.; Bach, G.; Dähne, S.; Kriwanek, J.; Lisk, M. *J. Prakt. Chem.* **1995**, *337*, 203.

(22) Pawlik, A.; Ouart, A.; Kirstein, S.; Abraham, H.-W.; Dähne, S. *Eur. J. Org. Chem.* **2003**, 3065.

(23) De Rossi, U.; Dähne, S.; Meskers, S. C. J.; Dekkers, H. P. J. M. *Angew. Chem.* **1996**, *108*, 827.

(24) Pawlik, A.; Kirstein, S.; De Rossi, U.; Dähne, S. *J. Phys. Chem. B* **1997**, *101*, 5646.

(25) Spitz, C.; Knoester, J.; Ouart, A.; Dähne, S. *Chem. Phys.* **2002**, *275*, 271.

(26) Lampoura, S. S.; Spitz, C.; Dähne, S.; Knoester, J.; Duppen, K. *J. Phys. Chem. B* **2002**, *106*, 3103.

(27) von Berlepsch, H.; Böttcher, C.; Ouart, A.; Burger, C.; Dähne, S.; Kirstein, S. *J. Phys. Chem. B* **2000**, *104*, 5255.

(28) Kirstein, S.; von Berlepsch, H.; Böttcher, C.; Burger, C.; Ouart, A.; Reck, G.; Dähne, S. *Chem. Phys. Chem.* **2000**, *1*, 146.

(29) von Berlepsch, H.; Böttcher, C.; Ouart, A.; Regenbrecht, M.; Akari, S.; Keiderling, U.; Schnablegger, H.; Dähne, S.; Kirstein, S. *Langmuir* **2000**, *16*, 5908.

(30) von Berlepsch, H.; Regenbrecht, M.; Dähne, S.; Kirstein, S.; Böttcher, C. *Langmuir* **2002**, *18*, 2901.

(31) von Berlepsch, H.; Kirstein, S.; Böttcher, C. *Langmuir* **2002**, *18*, 7699.

(32) von Berlepsch, H.; Kirstein, S.; Böttcher, C. *J. Phys. Chem. B* **2003**, *107*, 9646.

(33) von Berlepsch, H.; Kirstein, S.; Hania, R.; Didraga, C.; Pugžlys, A.; Böttcher, C. *J. Phys. Chem. B* **2003**, *107*, 14176.

(34) von Berlepsch, H.; Kirstein, S.; Böttcher, C. *J. Phys. Chem. B* **2004**, *108*, 18725.
(35) Didraga, C.; Pugžlys, A.; Hania, P. R.; von Berlepsch, H.; Duppen, K.; Knoester, J. *J. Phys. Chem. B* **2004**, *108*, 14976.
(36) According to the manufacturer, the extinction coefficients of the sulfonated derivatives are generally lower than those of the carboxylated derivatives.
(37) Ly, H. V.; Longo, M. L. *Biophys. J.* **2004**, *87*, 1013.
(38) Spitz, C.; Dähne, S.; Ouart, A.; Abraham, H. W. *J. Phys. Chem. B* **2000**, *104*, 8664.
(39) Pugžlys, A.; Augulis, R.; van Loosdrecht, P. H. M.; Didraga, C.; Malyshev, V. A.; Knoester, J. *J. Phys. Chem. B* **2006**, *110*, 20268.
(40) Gil, A.; Möbius, D.; Sández, I.; Suárez, A. *Langmuir* **2003**, *19*, 6430.
(41) Faul, C. F. J.; Antonietti, M. *Adv. Mater.* **2003**, *15*, 673.
(42) Norden, B. *J. Phys. Chem.* **1977**, *81*, 151.
(43) Aggeli, A.; Nyrkova, I. A.; Bell, M.; Harding, R.; Carrick, L.; McLeish, T. C. B.; Semenov, A. N.; Boden, N. *Proc. Natl. Acad. Sci. U.S.A.* **2001**, *98*, 11857.